Alternative black coatings prepared on aluminium alloy 1050

Christophe Casademont, Jérôme Roche, Laurent Arurault

Alternative black coatings prepared on aluminium alloy 1050

Christophe Casademont, Jérome Roche and Laurent Arurault

CIRIMAT, Université de Toulouse, CNRS, Université Toulouse 3 Paul Sabatier, Bât. CIRIMAT, Toulouse Cedex 9, France

ABSTRACT

The present study investigated the preparation and characterisation of alternative black anodic films on aluminium alloy 1050 using three different inorganic colouring processes. The colouring process was performed via the standard chemical reaction and two alternative mechanisms, i.e. electrochemical reaction or a combination of electrochemical and chemical reactions. Black anodic films with high thermo-optical properties ($\alpha_s \geq 0.90$ and $\varepsilon_n \geq 0.90$) were successfully obtained using all three processes. Differences in chemical content and location of the Co-based pigments in the coatings were highlighted and explained according to the colouring reaction mechanisms.

Introduction

A large number of black inorganic colouring processes have been or are now being developed, depending on the part design and the material used (e.g. metal alloy or carbon fibre reinforced polymer). For metals, black paints [1,2], electroless coatings [3–5], cathodic deposits [6], coloured anodic films [7] or micro-arc coatings [8–11] have thus been tested on copper [12], stainless steel [13], magnesium alloys [14,15], titanium alloys [16] and aluminium alloys (AAs). In particular, aluminium alloys are widely used due to their low density and high strength/weight ratio [17]. Black anodic films are usually prepared on aluminium alloys [18] by anodising the aluminium surface, followed by inorganic colouring based on the precipitation of CoS pigments. Goueffon et al. [19–23] extensively studied this black inorganic colouring process and highlighted in particular the punctual location of the black pigments, i.e. mainly at the top of the pores of the anodic films. This punctual location has a critical influence during thermal aging as for example when simulating a space environment, and explains the crazing and flaking phenomena, i.e. respectively crack formation and particle removal from the black coating.

The aim of the present work was to study alternative colouring processes to obtain new black anodic films, including black pigment located along the film thickness and showing high thermo-optical properties ($\alpha_s \geq 0.90$ and $\varepsilon_n \geq 0.90$). To this purpose, three colouring processes and the associated reaction mechanisms were studied: chemical colouring (i.e. the standard process), electrochemical colouring and electrochemical-

chemical colouring. The microstructure, chemical composition and thermo-optical properties of the resulting black coatings were evaluated, respectively, by FEG-SEM, Energy dispersive X-ray (EDX) profiles, absorptivity and emissivity measurements.

Experimental

Preparation processes

The substrate material used in this study was 1050 AA (99.5% Al, < 0.40% Fe, < 0.25% Si and < 0.05% Cu, wt-%), the size of the samples used being $45 \times 35 \times 1$ mm. AA 1050 was selected because is quite a pure alloy, allowing a model anodic film, showing an ordered porosity quite similar to the ideal microstructure described by Keller [24], to be prepared. The incorporation of the black pigments was therefore not limited by the tortuosity of the anodic film's porosity.

Preparation of the black anodic films required four main consecutive steps: surface pre-treatment (degreasing, pickling and desmutting), anodising, colouring and sealing.

Alloy sheets were degreased with ethanol, pickled in an alkaline bath (Na_2CO_3 (6.2 g L^{-1}) and an Na_3PO_4 (12.5 g L^{-1}) mixed aqueous solution at pH 11) for 5 min at 93°C. Finally, desmutting was performed in an acid bath (HNO_3 50%v/v) for 3 min at ambient temperature. The samples were rinsed using distilled water after each step.

The aluminium sheet was used as an anode and a lead plate ($60 \times 45 \times 1$ mm) as counter-electrode. Anodising was conducted in galvanostatic mode ($J_a = 1.2$ A dm^{-2}) using a sulphuric acid solution

(150 g L^{-1}) thermally regulated at 20°C and with moderate stirring (300 rev min^{-1}). The samples were immediately rinsed in distilled water after anodising. In order to study the influence of thickness on the colouring step, different anodising durations were performed (between 10 and 60 min).

In order to propose alternative colouring processes, three different colouring methods were then studied: chemical colouring (standard process), electrochemical colouring and electrochemical-chemical colouring.

The standard chemical colouring process (first process) is based on a chemical precipitation of CoS particles. The anodised sample was coloured by immersion in two successive baths. First, it was placed in a solution of cobalt acetate (200 g L^{-1}) regulated at 43 ± 2°C for 15 min to impregnate the pores then, second, the impregnated sample was dipped in a solution of ammonium sulphide (30 g L^{-1}) at room temperature for 10 min. A precipitation of CoS black pigments occurred in the porous anodic films as described by Goueffon et al. [19–23]. After each step, the samples were immediately rinsed in distilled water to remove the excess solution.

Electrocolouring of the anodic films (second process) was performed in a cell thermally regulated at 25 ± 2°C, using a cobalt plate as counter-electrode ($60 \times 45 \times 1$ mm). The electrolyte was made of cobalt sulphate (32 g L^{-1}), magnesium sulphate (20 g L^{-1}), ammonium sulphate (20 g L^{-1}) and boric acid (20 g L^{-1}). The process used alternating voltage at a frequency of 50 Hz for 5 min with applied effective voltages from 5 to 20 V (Blanc Electronique SA supply, type EA-4036). The samples were immediately rinsed in distilled water after electrocolouring.

The third process required two steps. The first involved an electrochemical reaction with a solution containing cobalt nitrate (32 g L^{-1}), magnesium sulphate (20 g L^{-1}), ammonium sulphate (20 g L^{-1}) and boric acid (20 g L^{-1}). It is important to note here that cobalt nitrate was used instead of cobalt sulphates for the electrocolouring electrolyte in the second colouring process. The electrochemical step was performed in an electrochemical cell thermally regulated (25 ± 2°C) using an alternating voltage (50 Hz) for 5 min, with different applied effective voltages. A cobalt plate counter-electrode ($60 \times 45 \times 1$ mm) was used. During the second step, the samples were dipped in a solution of ammonium sulphide (30 g L^{-1}) at room temperature for 10 min. The samples were immediately rinsed in distilled water to remove excess solution.

Each colouring step was followed by sealing of the samples in a mixed aqueous solution of nickel acetate (5 g L^{-1}) and boric acid (5 g L^{-1}) at 98 ± 2°C for 25 min so as to close the pores and protect the black pigments.

Characterisations

The microstructure of the films was observed by field-emission gun scanning electron microscopy (FEG-SEM-JEOL JSM6400) and SEM microscopy (JEOL JSM 6510). Film characteristics (i.e. thickness, average pore diameter and porosity) were evaluated by image analysis of FEG-SEM views using Image J software.

EDX spectroscopy analyses were conducted on the cross-section of the black anodic films in order to qualitatively determine the chemical composition inside the anodic film, and especially the location of the Co-based pigments.

Absorptivity measurements were performed using a solar spectrum reflectometer (Model SSR 6-Devices & Services Co. USA), while emissivity measurements were performed on a Model A1 emissometer from the same supplier.

Results and discussion

Before colouring, the anodising step was typically performed in galvanostatic mode for 60 min in a sulphuric acid bath (150 g L^{-1}, 20°C). The growth of the anodic film results from the electrochemical oxidation of the aluminium metal (Equation (1)), while its porosity mainly depends on the chemical dissolution (Equation (2)) occurring at its surface with the acidic electrolyte.

$$2Al + 3H_2O \rightarrow Al_2O_3 + 6H^+ + 6e^- \qquad (1)$$

$$Al_2O_3 + 6H^+ \rightarrow 2Al^{3+} + 3H_2O \qquad (2)$$
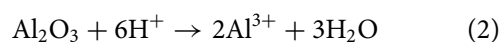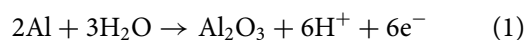
FEG-SEM cross-sectional views (Figure 1(a)) show that the standard anodic film has a thickness equal to 19 ± 1 µm (for 60 min), and includes straight cylindrical pores, perpendicular to the substrate. As expected, the porosity shows low tortuosity and the film microstructure is similar to the structure described by Keller's model [24]. FEG-SEM surface views (Figure 1(b)) highlight that the average pore diameter fluctuated from 2 to 25 nm (with an average value of 15 ± 2 nm), the porosity being about 36%.

The three types of black colouring were then studied in relation to the corresponding preparation processes. Microscopic and chemical analyses were performed, while the thermo-optical properties were evaluated and compared with the thermo-optical target values, i.e. absorptivity of 0.90 and emissivity of 0.90.

First process: standard chemical colouring

After chemical colouring and sealing, the resulting coloured standard film was of a dark black colour and showed no apparent cracks. Additional EDX analysis (Figure 2) showed the distribution of sulphur, cobalt and nickel along the cross-section of the coloured standard anodic film. The sulphur content
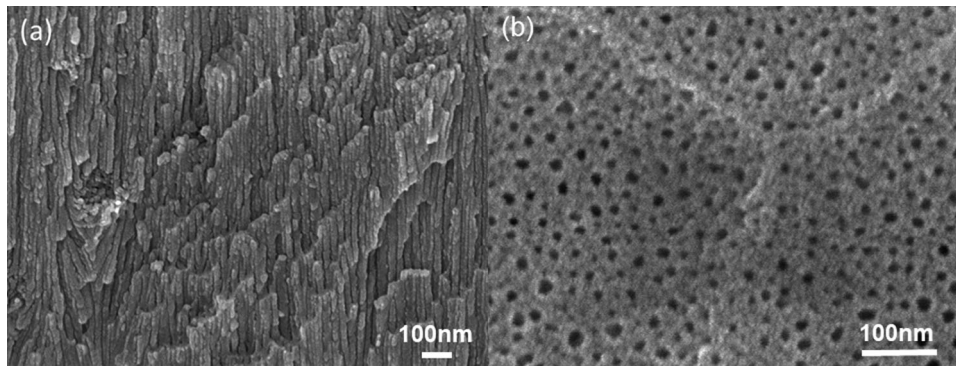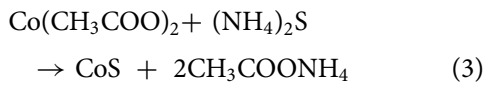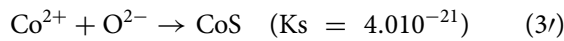
Figure 1. FEG-SEM (a) cross-sectional and (b) surface views of bare standard anodic film (20 μm thick) prepared on AA1050.

was higher at the top of the anodic film and decreased significantly toward the substrate. The presence of sulphur mainly in the upper part of the pores is explained by the reaction between sulphur and cobalt during the colouring and the formation of CoS (Equation (3)). This assumption was confirmed by the presence of a higher concentration of cobalt near the surface, down to 8 μm in depth.[25]

$$Co(CH_3COO)_2 + (NH_4)_2S$$
$$\rightarrow CoS + 2CH_3COONH_4 \quad (3)$$

or more simply

$$Co^{2+} + O^{2-} \rightarrow CoS \quad (Ks = 4.0 10^{-21}) \quad (3\prime)$$

The nickel element comes from the sealing step, occurring in quasi-boiling water (98 ± 2°C). Sealing involves both the formation of boehmite (Equation (4)) by the hydration of the anodic film, and the
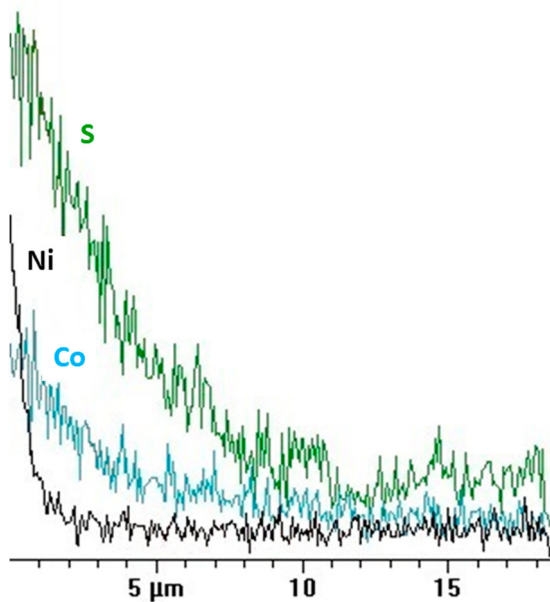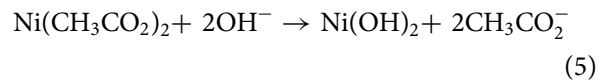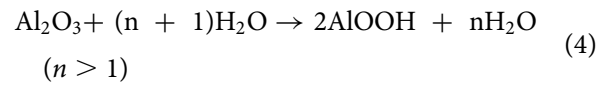
additional precipitation of nickel hydroxide (Equation (5)) from the nickel acetate additive.

$$Al_2O_3 + (n + 1)H_2O \rightarrow 2AlOOH + nH_2O$$
$$(n > 1) \quad (4)$$

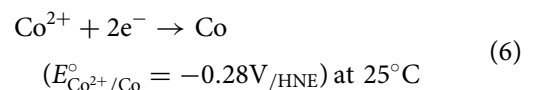$$Ni(CH_3CO_2)_2 + 2OH^- \rightarrow Ni(OH)_2 + 2CH_3CO_2^-$$
$$(5)$$

EDX analysis (Figure 2) shows that nickel was observed but only in the part closest to the surface (down to 3 μm inside the films), its penetration being limited by the presence of CoS pigments in the upper part of the pores. Resulting thermo-optical properties of the coloured standard film were 0.94 and 0.91 for absorptivity and emissivity, respectively.

Second process: electrochemical colouring

The objectives of this study into electrochemical colouring were threefold. The first goal was to obtain black anodic films, the second to determine the parameters that could affect electrochemical colouring and the last to determine optimum parameters.

Electrochemical colouring was performed using AC electrodeposition (50 Hz). Initially, the influence of the effective voltage on colouring and thermo-optical properties was evaluated through a preliminary study on 3.5 μm anodic films. Metal electrodeposition was observed from 7.5 V; a black colour was then obtained starting with 10 V whereas a deterioration of the surface was visually observed from 15 V (associated with gas release during the treatment). This work performed on 3.5 μm thick anodic film clearly highlights the impact of the applied voltage during electrodeposition. Electrodeposition, i.e. the reduction of cobalt ions (from cobalt sulphate) to cobalt metal (Equation (6)) [26–28], occurs during the cathodic part of voltage in AC mode and starts from a threshold bias voltage (here $U_t = 7.5$ V) [29].

Figure 2. EDX analyses of anodic film (20μm thick) on AA 1050, after standard chemical colouring and sealing.

$$Co^{2+} + 2e^- \rightarrow Co$$
$$(E^{\circ}_{Co^{2+}/Co} = -0.28V_{/HNE}) \text{ at } 25°C \quad (6)$$

At lower voltages ($U < U_t$) electrodeposition cannot occur, whereas for excessively high voltages ($U \geq 15$ V) reduction of the solvent occurs (Equation (7)), leading to the release of H_2 bubbles or an interfacial pH increase and so the possible precipitation of the cobalt hydroxide (Equation (8)).

$$2H_2O + 2e^- \rightarrow H_2 + 2OH^-$$
$$(E^\circ_{H_2O/H_2} = -0.83V_{/HNE}) \text{ at } 25°C \tag{7}$$

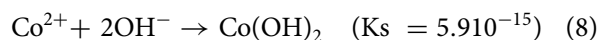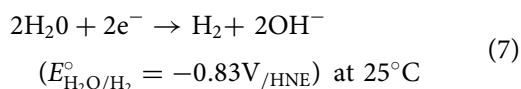$$Co^{2+} + 2OH^- \rightarrow Co(OH)_2 \quad (Ks = 5.9 \, 10^{-15}) \tag{8}$$

Figure 3 shows the results of absorptivity and emissivity for these different applied effective voltages (from 5 to 20 V). Thermo-optical properties responding to the required specifications for absorptivity ($\alpha_s = 0.90$) were obtained between 10 and 15 V. However, the emissivity values (Figure 3) were lower than the expected value ($\varepsilon_n = 0.90$). These differences are explained by the thinness (3.5 μm) of the anodic film used for this preliminary work. For greater thicknesses, the values of emissivity would probably be higher [21]. This effect of different thicknesses (3.5–20 μm) on emissivity is now studied, thermo-optical properties being evaluated for each case.

Visually, a black colour was thus obtained for thin films (3.5 and 4.7 μm), these results being confirmed by absorptivity measurements (Figure 4). The thermo-optical values also confirmed that the thickness has a significant influence on the emissivity of the samples. Indeed, the lowest value of emissivity (0.81) was obtained for a coating of 3.5 μm, whereas the highest value (0.92) was obtained for 19 μm (Figure 4). EDX analysis (Figure 5) shows similar distribution of S and Ni in the cross-section of the anodic film for different thicknesses (5, 10 and 20 μm). Meanwhile, the cobalt is mainly located near the bottom of the anodic film, i.e. near the interface with the compact layer.

To summarise, the black anodic film showing optimal thermo-optical properties was obtained on AA 1050 for a thickness of 9.7 ± 0.3 μm and for an applied
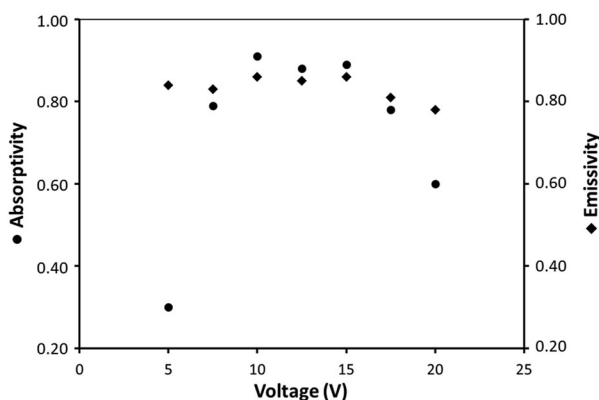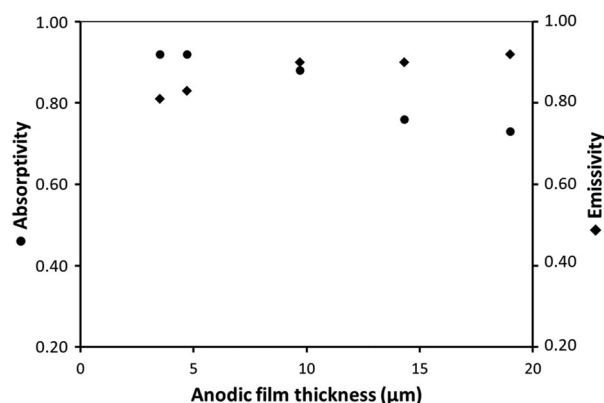

Figure 4. Absorptivity and emissivity values of anodic films (with different thicknesses) prepared on AA1050 after electro-colouring (effective voltage U = 10 V) and sealing.

voltage of 10 V during electrochemical colouring treatment.

Third process: electrochemical – chemical colouring

One aim of the present study was to develop an alternative colouring process to prepare black anodic films, having black pigments all along the pores. The new process included both an electrochemical step and a chemical step. It is important to recall that cobalt nitrate was used instead of cobalt sulphate for the electrocolouring electrolyte in the second colouring process.

The influence of the effective voltage applied during the electrochemical step was the first parameter evaluated. A study was conducted on anodic films of 5 μm for applied effective voltages varying from 5 to 15 V during the electrochemical step, while the impregnation in $(NH_4)_2S$ was kept constant for 10 min. Following the electrochemical step, no black colouring was visually observed whatever the applied effective voltage; rather a blue/grey colour was obtained. These results demonstrate the absence of cobalt electrodeposition in the cobalt nitrate solution, unlike the results obtained after electrochemical colouring in cobalt sulphate electrolyte. Indeed, due to their respective standard potentials (E° NO_3^-/NO_2^- = + 0.01 V/HNE and E° Co^{2+}/Co = –0.28 V/HNE, at 25°C), the reduction of nitrate (Equation (9)) occurs before the reduction of cobalt ions (Equation (6)). Instead of metal deposition, hydroxide ions were electrogenerated and subsequently reacted with cobalt ions (Equation (8)) inducing the precipitation of cobalt hydroxide $Co(OH)_2$.

$$NO_3^- + H_2O + 2e^- \leftrightarrow NO_2^- + 2OH^-$$
$$(E^\circ_{NO_3^-/NO_2^-} = +0.01V_{/HNE}) \text{ at } 25°C \tag{9}$$
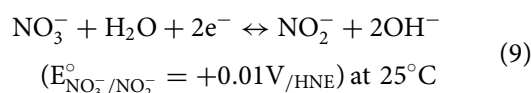
This reaction can explain the absence of black colour after electrochemical treatment since cobalt had

Figure 3. Absorptivity and emissivity values of anodic films (3.5 μm thick) prepared on AA1050 for different electrocolouring voltages.
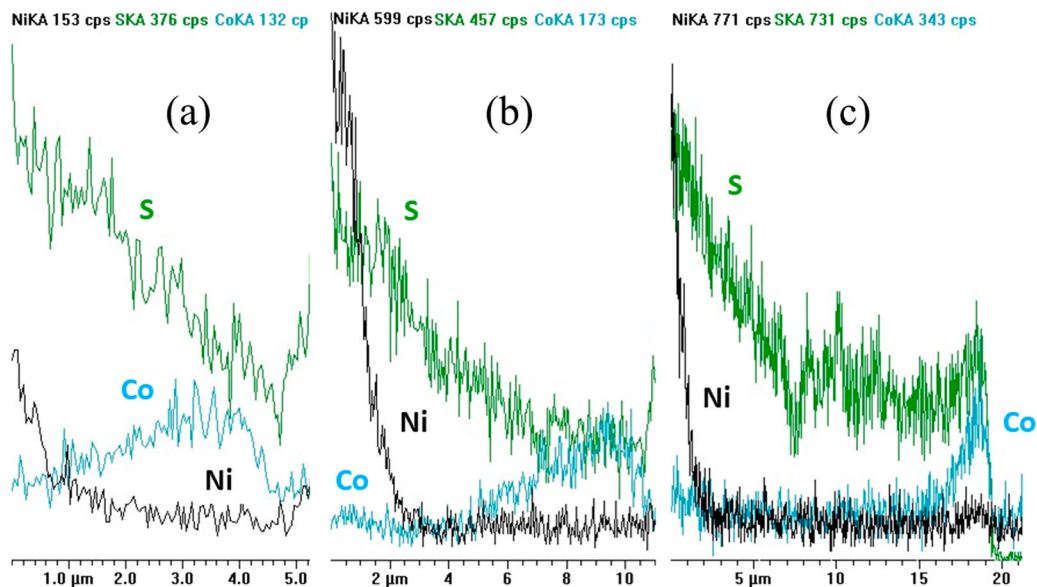
Figure 5. EDX analyses of electrocoloured and sealed anodic films prepared on AA1050, showing different thicknesses (i.e. (a) 5 μm, (b) 10 μm, (c) 20 μm).

reacted to form $Co(OH)_2$ before reduction to cobalt. The blue/grey colour obtained concurs with the presence of $Co(OH)_2$ as previously reported by Lide and Haynes [25], while the colour of Co_3O_4, the other oxide that could be potentially formed in the presence of nitrates, has been reported as being black [28,30].

After electrochemical treatment, the samples were then immersed for 10 min in ammonium sulphide $((NH_4)_2S; 30\,g\,L^{-1})$ at room temperature. After this second step, no significant differences were observed (i.e. the blue/grey appearance remained), except for the case with an applied voltage of 5 V where the sample had a grey hue. Thermo-optical properties were also checked (Figure 6); as for visual observations, no significant differences appeared for absorptivity (from 0.63 to 0.67) between 7.5 and 15 V, the lowest value being 0.42 for 5 V. Neither were any differences observed for emissivity (in the 0.80–0.84 range).
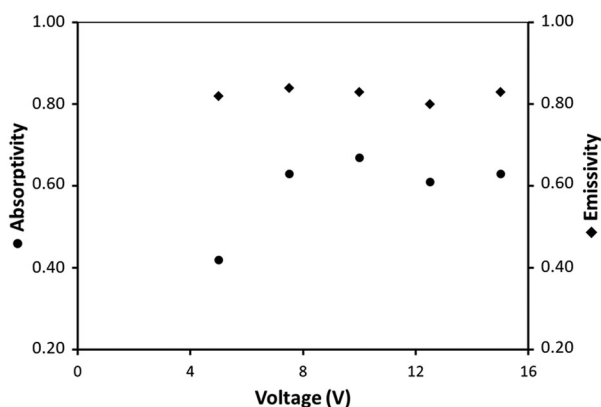
However, the results of this preliminary parametric study did not allow the required thermo-optical properties ($\alpha_s \geq 0.90$ and $\varepsilon_n \geq 0.90$) to be obtained.

To improve this third colouring process, experiments were performed for different film thicknesses, i.e. from 5 to 30 μm. The voltage applied during the electrochemical step was kept constant at 10 V, while impregnation in ammonium sulphide was conducted for 10 min. A black colour was visually observed for the samples with a thickness equal to or above 20 μm, the corresponding thermo-optical properties confirming these results since absorptivity was 0.83 for a thickness greater than 20 μm and above 0.90 for a thickness of 30 μm (Figure 7). Additional EDX analysis (Figure 8) conducted into the depth of the anodic films (10, 20 and 30 μm thick) show that sulphur and cobalt elements are both present, although the latter only appears in small quantities. This simultaneous

Figure 6. Absorptivity and emissivity values for anodic films (5 μm thick) prepared on AA1050, after electrochemical – chemical colouring and sealing; the first electrochemical step is performed using different effective voltages, while impregnation in $(NH_4)_2S$ lasts 10 min.
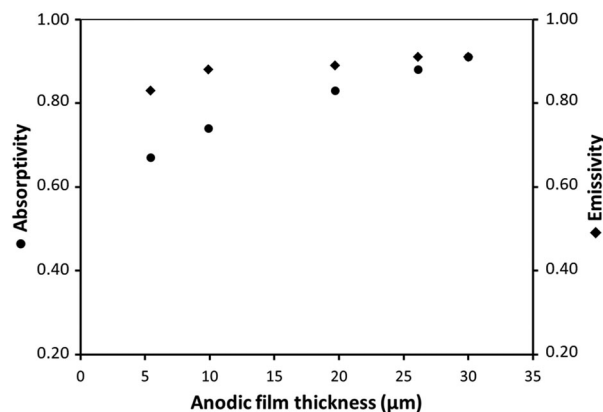

Figure 7. Absorptivity and emissivity values of anodic films (with different thicknesses) prepared on AA1050, after electrochemical – chemical colouring and sealing; the first electrochemical step is performed using 10 V, while impregnation in $(NH_4)_2S$ lasts 10 min.
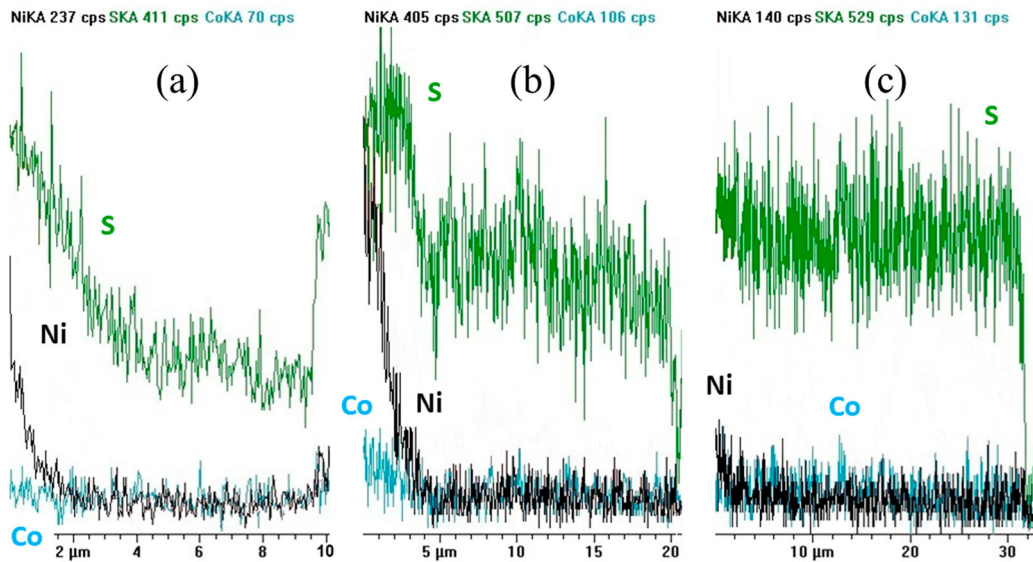
Figure 8. EDX analyses of anodic films prepared on AA 1050 with different thicknesses ((a) 10 μm, (b) 20 μm, (c) 30 μm), after electrochemical – chemical colouring and sealing.

presence of both elements during this second chemical step of the third process could be explained by the formation of cobalt sulphide (CoS). Indeed, considering their respective constants of solubility at 25°C (Ks of $Co(OH)_2 = 5.9 \ 10^{-15}$ and Ks of $CoS = 4.0 \ 10^{-21}$ [21]), the displacement of the hydroxides by the sulphides and the subsequent precipitation of CoS black pigments could occur in the pores as described in Equation (10):

$$Co(OH)_2 + (NH_4)_2S \rightarrow CoS + 2NH_4OH \quad (10)$$
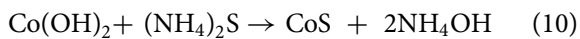
The study showed that it was possible to prepare black anodic film forming first $Co(OH)_2$ inside the pores during the electrochemical step, and then replace this component with CoS during the chemical reaction; however, the thermo-optical properties α_s obtained were insufficient with regard to the expected values ($\alpha_s > 0.90$) when the thickness was lower than 30 μm. To improve this process for lower thickness values (e.g. 20 or 25 μm), a further study was conducted on the impact of the impregnation time (20 and 30 min) in sulphide ammonium. Visual inspection shows that an increase in the impregnation time improves the colouring process, since a black colour was obtained for each case. By contrast, emissivity did not appear to

be affected significantly by the treatment times (0.89 and 0.91 for 20 and 25 μm, respectively). However, this operational parameter did impact absorptivity, which increased with a treatment time of 20 min, although the effect became negligible after 30 min for each thickness (Table 1). Thus, the desired thermo-optical properties (i.e. $\alpha_s = 0.93$ and $\varepsilon_n = 0.91$) can also be obtained for lower thicknesses, for instance, 25 μm.

Conclusion

Three processes used to colour anodic films prepared on AA 1050 were investigated. A standard process involving a chemical colouring was compared with two alternative processes using either an electrochemical or an electrochemical-chemical colouring. According to the specific experimental conditions (i.e. coating thickness, duration and effective voltage of the treatment), black anodic films with expected properties ($\alpha_s \geq 0.90$ and $\varepsilon_n \geq 0.90$) were obtained for each colouring process. The main difference between the three processes was seen to be in the chemical composition and the location of Co-based pigments. For the chemical colouring involving CoS, black precipitates occurred mainly in the upper part of the pores, whereas the cobalt metal obtained by electrochemical colouring was located at the bottom of the anodic film. Finally, the electrochemical-chemical colouring would have to be more uniform since Co-based particles appeared distributed all along the pores. This feature could allow good thermo-optical properties to be maintained after partial wear of the coating and would appear to offer truly interesting alternatives to industrial colouring applications, e.g. for passive thermal control of spacecraft or low-cost solar absorber manufacturing.

Table 1. Absorptivity values for anodic films ((a) 20 and (b) 25 μm) prepared on AA1050 after electrochemical – chemical colouring and sealing; the first electrochemical step is performed using 10 V, the second chemical step is an impregnation in $(NH_4)_2S$ solution for different durations.

Duration of impregnation (min)	10	20	30
Absorptivity (α_s) for an anodic films of 20 μm	0.83	0.87	0.88
Absorptivity (α_s) for an anodic films of 25 μm	0.88	0.91	0.93

ORCID

Laurent Arurault http://orcid.org/0000-0003-2364-2236

References

[1] Ramaseshan K, Viswanathan M, Thutupalli GKM. Optical black coatings for space applications. Bull Mater Sci. 1986;8(5):581–586.

[2] Holtzclaw KW, Fraser ME, Gleb A, et al. Infrared emission from reactions of high-velocity atomic oxygen with black surfaces: Z306 paint, anodized aluminum, and Teflon. Appl Opt. 1994;33(22):5062–5067.

[3] Rani R U, Sharma AK, Mayanna SM, et al. Black permanganate conversion coatings on aluminium alloys for thermal control of spacecraft. Surf Eng. 2005;21(3):198–203.

[4] Saxena V, Uma Rani R, Sharma AK. Studies on ultra high solar absorber black electroless nickel coatings on aluminum alloys for space application. Surf Coat Technol. 2006;201:855–862.

[5] Selvam M. Colouring of anodized aluminium by electroless method. Surf Eng. 2011;27(9):711–718.

[6] Jeeva PA, Narayanan S, Karthikeyan S. A review on black coatings for solar energy storaging systems. Inter J ChemTech Res. 2016;9(3):589–596.

[7] Sharma AK, Uma Rani R, Malek A, et al. Black anodizing of a magnesium-lithium alloy. Met Finish. 1996;94:16–27.

[8] Wang L, Zhou J, Liang J, et al. Thermal control coatings on magnesium alloys prepared by plasma electrolytic oxidation. Appl Surf Sci. 2013;280:151–155.

[9] Yao Z, Xia Q, Shen Q, et al. A facile preparation of ceramic coatings on Ti alloys for thermal protection systems. Sol Energ Mater Sol C. 2015;143:236–241.

[10] Arunnellaiappan T, Rama Krishna L, Anoop S, et al. Fabrication of multifunctional black PEO coatings on AA7075 for spacecraft applications. Surf Coat Technol. 2016;307:735–746.

[11] Wu X, Qin W, Cui B, et al. The influence of the oxidation time on the optical properties of the ceramic thermal control coating prepared by micro-plasma oxidation. J Mater Sci. 2007;42:7251–7255.

[12] Somasundaram S, Pillai AM, Sharma AK. High emittance black nickel coating on copper substrate. J Alloy Compd. 2015;643:263–269.

[13] Maria Shalini V, Arockiasamy P, Uma Rani R, et al. Flat absorber phosphorous black nickel coatings for space applications. J Mater Sci Technol. 2012;28(2):118–124.

[14] Sharma AK, Uma Rani R, Mayanna SM. Thermal studies on electrodeposited black oxide coating on magnesium alloys. Thermochim Acta. 2001;376:67–75.

[15] Parida B, Uma Rani R, Sharma AK. Studies on chrome free galvanic conversion coating on magnesium alloy AZ31B for space applications. Surf Eng. 2010;26(5):361–366.

[16] Uma Rani R, Sharma AK, Minu C. Studies on black electrolesss nickel coatings on titanium alloys for spacecraft thermal control applications. J Appl Electrochem. 2010;40:333–339.

[17] Uma Rani R, Subba Rao Y, Sharma AK. Studies on black anodic coatings for spacecraft thermal control applications. Galvanotechnik. 2011;109:2182–2189.

[18] Sharma AK, Bhojraj H, Kaila VK, et al. Anodizing and inorganic black coloring of aluminium alloys for space applications. Met Finish. 1997;95:14–20.

[19] Goueffon Y, Arurault L, Mabru C, et al. Black anodic coatings for space applications: study of the process parameters, characteristics and mechanical properties. J Mat Process Technol. 2009;209:5145–5151.

[20] Goueffon Y, Mabru C, Labarrère M, et al. Mechanical behavior of black anodic films on 7175 aluminium alloy for space application. Surf Coat Technol. 2009;204:1013–1017.

[21] Goueffon Y, Arurault L, Fontorbes S, et al. Chemical characteristics, mechanical and thermo-optical properties of black anodic films prepared on 7175 aluminium alloy for space application. Mat Chem Phys. 2010;120:636–642.

[22] Goueffon Y, Mabru C, Labarrère M, et al. Investigations into the coefficient of thermal expansion of porous films prepared on AA7175 T7351 by anodizing in sulphuric acid electrolyte. Surf Coat Technol. 2010;205:2643–2648.

[23] Goueffon Y, Aldebert G, Mabru C, et al. Flaking of black anodic films in space environment: ageing and numerical simulation. Mech Mater. 2012;45:72–82.

[24] Keller F, Hunter MS, Robinson DL. Structural features of oxide coatings on aluminium. J Electrochem Soc. 1953;100:411–419.

[25] Lide DR, Haynes M. Handbook chemistry and physics 90th. Boca Raton: CRC Press; 2010; p. 8–127.

[26] Arurault L, Salmi J, Bes RS. Comparison of AC voltage and periodic-reverse current nickel pigmented anodized aluminium as solar selective absorber. Sol Energ Mater Sol C. 2004;82:447–455.

[27] Zemanová M, Chovancová M, Gáliková Z, et al. Nickel electrolytic colouring of anodic alumina for selective solar absorbing films. Renew Energ. 2008;33:2303–2310.

[28] Barrera E, Gonzales I, Viveros T. A new cobalt oxide electrodeposit bath for solar absorbers. Sol Energ Mater Sol C. 1998;51:69–82.

[29] Arurault L, Bes RS. Kinetics of metallic electrochemical impregnation of porous anodic oxidation layer on 1050 and 2024 aluminium alloys. Adv Engin Mat. 2003;5:433–435.

[30] Barrera CE, Lara H, Viveros GT, et al. Degradation study of black cobalt coating. Surf Eng. 2000;16(1):50–53.